

RESEARCH ARTICLE

Cytotoxic study of green synthesized pure and Ag-doped $\alpha\text{-Fe}_2\text{O}_3$ nanoparticles on breast cancer (MCF-7) cell line

Amir Abbas Esmailzadeh¹, Soheil rasoolzadegan², Ali Reza Arabi³, Dadkhoda Soofi⁴, Seyed Saied Rajaei Ramsheh⁵, Wasan Saad Ahmed⁶, Raziye Moaref Pour^{7*}

¹ Salamat yar behesht dayan ,Dayan biotech company , Tehran, Iran

² Department of Neurology, School of Medicine, Shahid Beheshti University of Medical Sciences, Tehran, Iran

³ Centre for processing and characterization of nanostructured materials, School of mechanical engineering, University of Tehran, Tehran Iran

⁴ Internal of Medicine, Faculty Member, Department of Medicine, Zabol University of Medical Sciences, Zabol, Iran

⁵ Clinical Research Development Unit, Hajar Hospital, Shahrekord University of Medical Sciences, Shahrekord, Iran

⁶ Department of Computer Science, Al-Turath University College, Al-Mansour, Baghdad, Iraq

⁷ Department of Oral and Maxillofacial surgery, School of Dentistry, Ahvaz Jundishapur University of Medical Sciences, Ahvaz, Iran

ARTICLE INFO

Article History:

Received 01 Sep 2022

Accepted 20 Oct 2022

Published 01 Nov 2022

Keywords:

Ag-doped $\alpha\text{-Fe}_2\text{O}_3$
nanoparticles

Iron oxide nanoparticles

silver nanoparticles

breast cancer

ABSTRACT

In this research attempted to prepare hematite ($\alpha\text{-Fe}_2\text{O}_3$) and silver doped hematite nanoparticles (Ag-doped $\alpha\text{-Fe}_2\text{O}_3$ NPs) by using the aqueous extract of *Prosopis farcta* fruit. The synthesized NPs were identified through the results of X-ray Diffraction (XRD), Field Energy Scanning Electron Microscopy (FESEM), Raman, Energy Dispersive X-ray (EDX), and Vibrating Sample Magnetometer (VSM) technics. Accordingly, the NPs contained a spherical shape with a size range of 40-50 nm. Also, we surveyed their cytotoxic against human breast cancer (MCF-7) cell line, which showed a potential functionality at the concentration of 80 $\mu\text{g}/\text{mL}$. Therefore, the synthesized NPs can be proposed as an applicable candidate for medical applications.

How to cite this article

Esmailzadeh A.A., Rasoolzadegan S., Arabi A.R., Soofi D., Rajaei Ramsheh S.S., Saad Ahmed W., Moaref pour R. Cytotoxic study of green synthesized pure and Ag-doped $\alpha\text{-Fe}_2\text{O}_3$ nanoparticles on breast cancer (MCF-7) cell line. *Nanomed Res J*, 2022; 7(4): 370-377. DOI: 10.22034/nmrj.2022.04.007

INTRODUCTION

The science of nanotechnology has helped in facilitating the diagnosis and treatment of diseases [1, 2]. Magnetic nanoparticles proved to contain a great ability for improving the diagnosis and cure of various illness, especially cancer [3, 4]. Their application as contrast enhancers in conventional magnetic resonance imaging, as well as nanocarriers in modern drug delivery systems, attracted the interest of many researchers in recent years.

Valuable and desirable results were achieved by the performed assessments on the targeted transfer of chemotherapy agents to cancer cells with the help of magnetic nanoparticles throughout *in vitro* and *in vivo* conditions [3]. In addition, these particles were exerted for the treatment of cancer through the method of heating, as well as in the transferring of nucleic acids, plasmids, and siRNA to cells [3].

Providing the early-stage diagnosis of diseases is a very important factor in the improvement of treatment methods. Nowadays, the exerted

* Corresponding Author Email: rmoarefpour@gmail.com

treatments for the diagnosis of cancer are usually based on detecting the induced changes in cells and tissues, which can be also conducted by clinical trials and conventional imaging techniques [5]. However, the goal of scientists is to succeed in identifying cancer upon the occurrence of the first molecular changes [5-8]. Iron oxide nanoparticles are currently the only magnetic nanomaterials that are used as a carrier in drug delivery and a contrast agent in clinical medicine for magnetic resonance imaging [3]. According to the performed experiments on iron oxide nanoparticles over several years, these particles do not cause any immediate or long-term toxic effects on the body and also, their functionality on cells can be enhanced by the presence of certain nanoparticles with nanocarriers [3].

Breast cancer is the important type of cancer in womenfolk [9, 10]. The available common cancer cure involved radiation therapy, surgery, and chemotherapy, that often result in annihilating the healthy cells, while causing the risk of toxic impacts and side effects [10]. In recent years, the lack of radiotherapy and chemotherapy for the progressive forms of cancer, it is necessary to discover new techniques to control cancer, which is one of the applications of NPs, especially iron oxide nanoparticles [11].

In recent years, a lot of attention was invested in the synthesis of nano-sized iron particles due to their extended capabilities as a result of increasing their surface area and surface activity in nanoscale [12-16]. Considering the importance of iron oxide nanoparticles in medical and non-medical fields, researchers attempted the production of these nanoparticles through green synthesizing methods. Iron oxide nanoparticles are widely exerted as catalysts and sensors, as well as for magnetic storage and drug delivery implementations [17].

Biosynthesizing techniques that implicate the usage of plant extracts are simple, efficient, cost-effective, and applicable approaches that can stand as suitable alternatives to conventional preparation methods for increasing the production of nanoparticles [18]. Plants contain biomolecules such as carbohydrates, proteins, and coenzymes that can provide a great potential for reducing metal salts into nanoparticles and maintain their stabilization [18]. Therefore, this study attempted to synthesize pure and Ag-doped α -Fe₂O₃ NPs through aqueous extract of *Prosopis farcta* fruit, and in the following examined their cytotoxic activity on breast cancer cell line.

MATERIALS AND METHOD

prepare of Prosopis farcta

The fruit of *P. farcta* was acquired, washed, and dried at room temperature to be powdered and weighed. Then, distilled water was added to the fruit powder in the ratio of 10:1 to be shaken for 10 h. The mixture filtered and resulted extract was exerted for the synthesis of nanoparticles.

prepare of α -Fe₂O₃ NPs

To start the prepare of Fe₂O₃ NPs, 15 mL of extract was volumed to 50 mL with distilled water. Then, iron (III) chloride (FeCl₃, 1M) solution was added to the extract and stirred at 80 °C for 4 h. Once the pH of solution was regularized to 11 using sodium hydroxide (NaOH, 1 M, Merck) solution, the resulting mixture dried at 90 °C. The resulted powder calcined at 500 °C for 1:30 h to achieve the powder nanoparticles of iron oxide.

prepare of Ag-doped α -Fe₂O₃ NPs

For the synthesis of Ag-doped α -Fe₂O₃, 15 mL of the extract taken at 70 °C of water bath to be afterwards volumed to 50 mL by distilled water. Then, FeCl₃ (0.1 M, Merck) was adjoined to extract solution. After a few minutes, silver nitrate (Ag(NO₃), 0.025 M, Merck) was added and mixed with the reaction container for 2 h at 75 °C. Once the pH of solution was compatible by usage of sodium hydroxide (NaOH, 1M, Merck, pH=11), obtained solution placed in oven at 90 °C for 12 h. Subsequent to being dried, the resulted precipitate was calcinated at 500 °C for 1:30 h to achieve brown powder of Ag-dop- α -Fe₂O₃ NPs.

Cytotoxic test

Breast (MCF-7) cancer cells purchased from the Pasteur Institute (Tehran, Iran) for toxicity assessment of α -Fe₂O₃ and Ag-doped α -Fe₂O₃ nanoparticles. The cells cultured in DMEM (4.5 g/L) with 10% (v/v) FBS, 100 mg/mL of streptomycin, and 100 units/mL of penicillin within a CO₂ (5% CO₂, 37 °C) incubator. The cells were taken into culture plates until to reaching 80% of growth. On the next day, diverse concentrations of NPs (5-320 μ g/mL) were separately added and then, the cells were incubated at 37 °C for 24 h. After the incubation completed, MTT solution in PBS (5 mg/mL) added to each well and another incubation process was performed for 3 h at 37 °C. The absorbance (Abs) of dissolved formazan was evaluated at 570 nm using plate reader (Stat FAX303). The outcomes reported

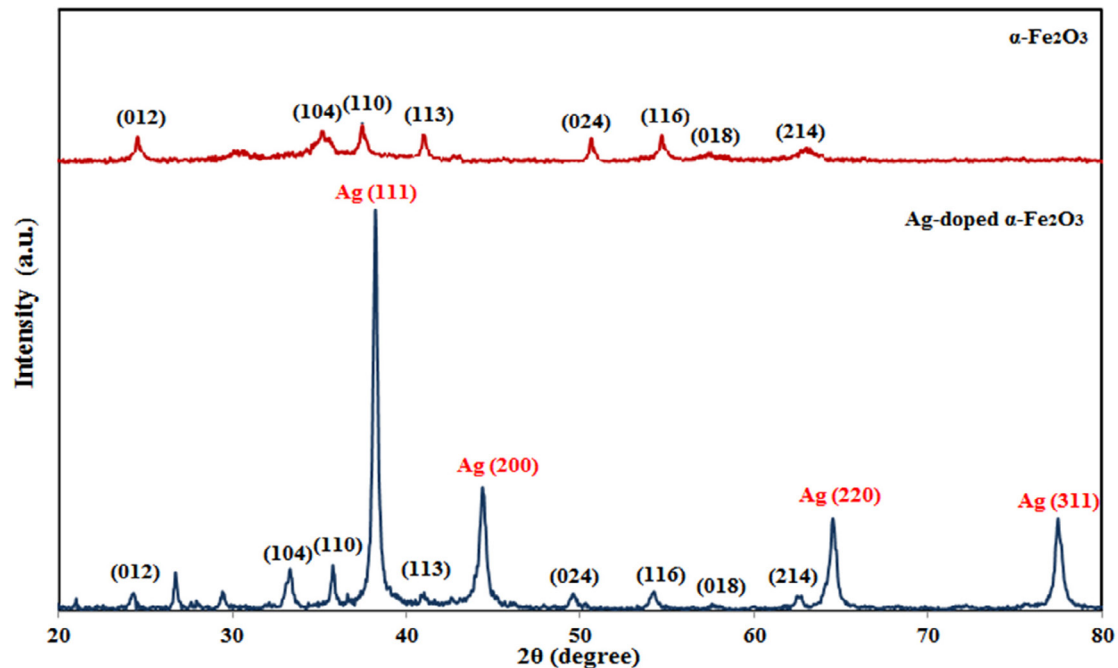


Fig. 1. XRD spectra of pure and Ag-dop- α -Fe₂O₃ NPs

as mean \pm SD. The viability of cured cells estimated by the below equation.

$$\text{Viability (\%)} = (\text{Abs of treated cells} / \text{Abs of control}) * 100$$

RESULTS AND DISCUSSION

XRD

The x-ray diffraction of α -Fe₂O₃ and Ag-doped α -Fe₂O₃ NPs are showed in Fig. 1. The diffraction pattern of α -Fe₂O₃ exhibited peaks in the 2θ positions of 25.21, 34.12, 35.58, 41.18, 49.51, 53.71, 58.86, and 61.28° that were related to the (021), (104), (110), (113), (024), (116), (018), and (214) planes. These Miller indices indicated the presence of hematite nanoparticles (α -Fe₂O₃) (JCPDS card no. 39-1346) [4]. According to Fig. 1, the diffraction pattern of Ag-doped α -Fe₂O₃ NPs displayed some additional peaks in the 2θ position of 38.1, 43.2, 65.4, and 72.1°, which implied the presence of silver atom throughout the crystalline structure of doped NPs. Based on the detected diffraction peak at $2\theta = 35.58^\circ$, the crystalline particle size of α -Fe₂O₃ was calculated by the usage of Debye-Scherrer's equation be 34.50 and 41.59 nm for α -Fe₂O₃ and Ag-doped α -Fe₂O₃ NPs, respectively. According to the comparison between the ion radius of silver

(1.26 Å) and Fe (0.645 Å), the crystalline size of doped nanoparticles was larger than the pure nanoparticles.

FESEM and EDX

The particle size and morphology of synthesized pure and Ag-dop- α -Fe₂O₃ NPs observed through the SEM images (Fig. 2). Accordingly, pure and doped nanoparticles contained a spherical shape and the particle sizes of 40 and 50 nm for pure and Ag-dop- α -Fe₂O₃ NPs, respectively. In conformity to Fig. 2, the doping of silver into the hematite structure resulted in reducing the particle size, which was also indicated by PXRD findings. The EDX outcomes are presented in Fig. 3, which clearly certifies the presence of doped silver in the nanoparticles.

Raman

The Raman of synthesized pure and Ag-dop- α -Fe₂O₃ NPs exhibited at Fig. 4. Raman spectrum of α -Fe₂O₃ NPs displayed bands at 296, 414, and 667 cm⁻¹. The bands at 296 and 414 cm⁻¹ are in correspondence to phonon A_{1g} and E_g modes. Peak at 667 cm⁻¹ depended to the attendance of iron oxide NPs. The Raman diagram of Ag-dop- α -Fe₂O₃ NPs displayed the appearance of a peak at 598 cm⁻¹,

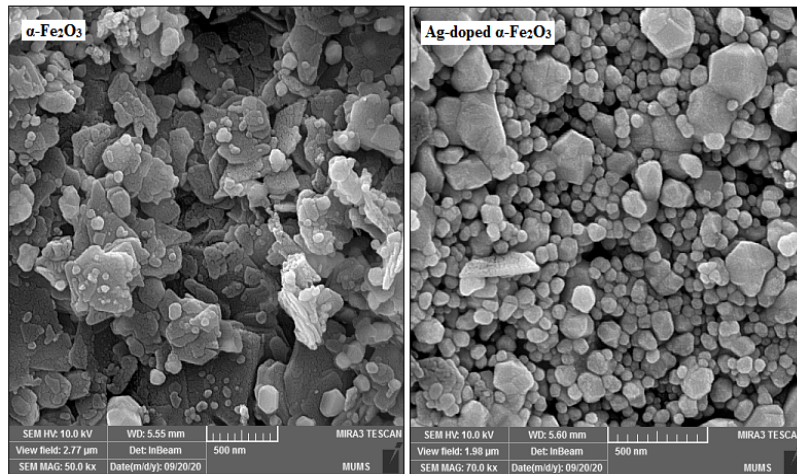


Fig. 2. FESEM spectra of pure and Ag-dop- $\alpha\text{-Fe}_2\text{O}_3$ NPs

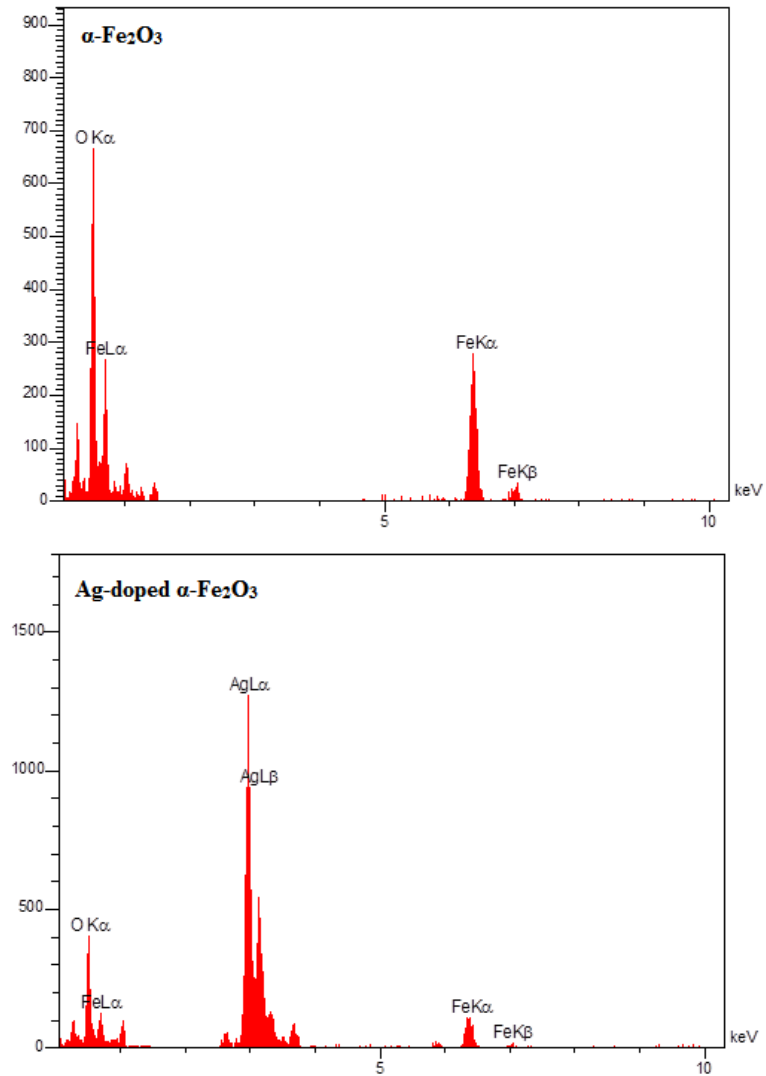


Fig. 3. EDX spectra of pure and Ag-dop- $\alpha\text{-Fe}_2\text{O}_3$ NPs

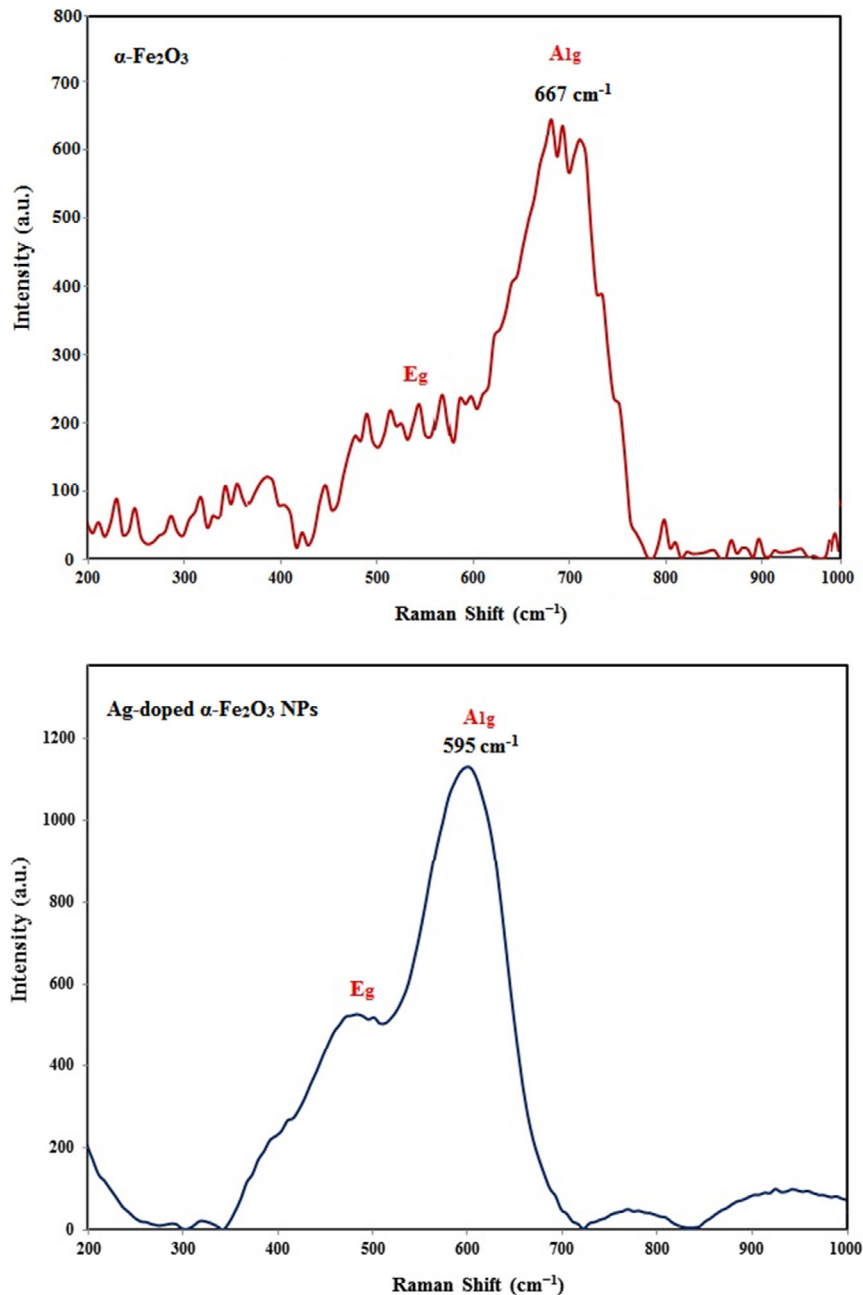


Fig. 4. Raman of pure and Ag-dop- $\alpha\text{-Fe}_2\text{O}_3$ NPs

which was attributed to A_{1g} mode and signified the $\alpha\text{-Fe}_2\text{O}_3$ sample. According to previous study [12], the Raman spectrum exhibited two modes for the $\alpha\text{-Fe}_2\text{O}_3$ nanoparticles including A_{1g} (595 cm^{-1}) and E_g (422 cm^{-1}), while the observed shift throughout the graph was pertinence to the presence of silver in the sample's structure.

VSM

The magnetic effect of the synthesized pure and Ag-dop- $\alpha\text{-Fe}_2\text{O}_3$ NPs investigated through results of VSM technique (Fig. 5). As it is displayed in Fig. 5, the magnetic saturation (M_s) of $\alpha\text{-Fe}_2\text{O}_3$ NPs was 1.5 emu/g . According to similar work, $\alpha\text{-Fe}_2\text{O}_3$ contained a magnetic saturation (M_s)

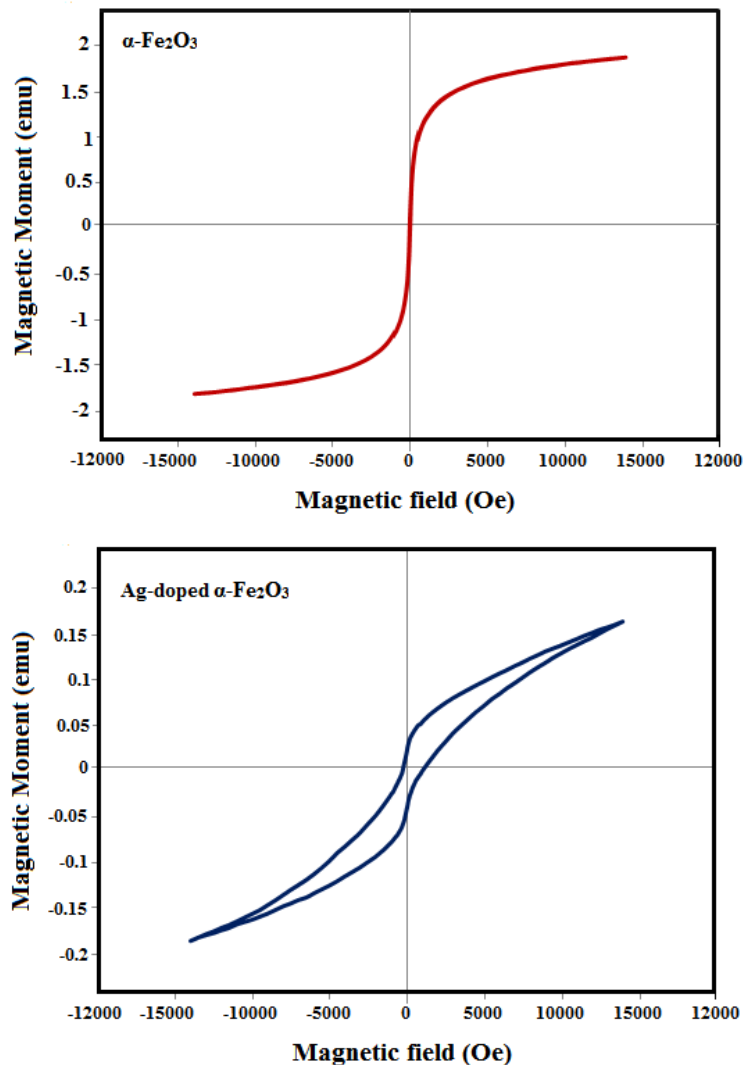


Fig. 5. VSM of pure and Ag-dop- $\alpha\text{-Fe}_2\text{O}_3$ NPs

value of 1.8 emu/g [12]. The small hysteresis loop of $\alpha\text{-Fe}_2\text{O}_3$ NPs is indicative of its superparamagnetic behavior. Since paramagnetic substances are a type of soft magnetic, their easy magnetization, they rapidly miss their magnetic moments upon the removal of applied magnetic field [19]. According to the survey of Bepari *et al* on the magnetic effect of Fe_2O_3 NPs, the Ms content of these NPs has a straight linkage to their particle size and shape anisotropy [20]. The saturation magnetization of Ag-dop- $\alpha\text{-Fe}_2\text{O}_3$ NPs was determined to be 0.16 emu/g (Fig. 5). Apparently, the presence of silver in the structure of nanoparticles caused a decrease in the saturation magnetization of samples.

Cytotoxic performance

We studied the cytotoxic activity of pure and Ag-dop- $\alpha\text{-Fe}_2\text{O}_3$ NPs on MCF-7 using a MTT test. MTT, as a determinant of cytotoxicity and cell viability, was estimated to assign the rate of cellular metabolic performance in cured mitochondria cells. This test was functioned with the NPs concentrations of 0-200 $\mu\text{g}/\text{mL}$ in 24 h of treatment time (Fig. 6). Based on Fig. 6, the cytotoxic of synthesized pure and Ag-dop- $\alpha\text{-Fe}_2\text{O}_3$ NPs on the cancer cell of MCF-7 were observed at the concentrations of 320 and 80 $\mu\text{g}/\text{mL}$. Accordingly, the Ag-dop- $\alpha\text{-Fe}_2\text{O}_3$ NPs were able to annihilate 50% of the cells and performed a complete

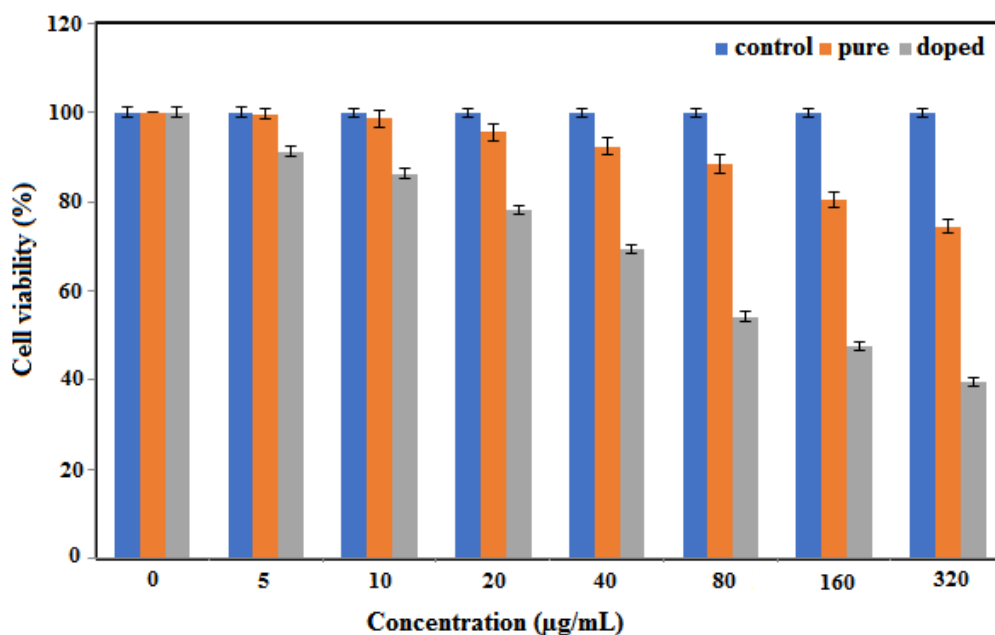


Fig. 6. Cytotoxic activity of pure and Ag-doped α -Fe₂O₃ NPs on MCF-7 cell line.

annihilation at concentrations above 80 $\mu\text{g/mL}$. Fig. 6 depicts the conditions of normal and cancer cells before and after being treated with the synthesized nanoparticles in different concentrations. The toxicity effects of synthesized nanoparticles can be clearly perceived, which resulted in the destruction and death of cells.

The potential cytotoxicity of nanoparticles is caused by their ROS or Reactive oxygen species [21]. Therefore, oxidative stress can be an applicable scale for comparing the toxic effects of nanoparticles [22]. According to most of the related studies, iron oxide nanoparticles at the concentration range of 100 $\mu\text{g/mL}$ and above can cause toxic effects on different cell lines [23], which is consistent with the outcomes of this work. Metal nanoparticles can produce toxins in human tissues and cell cultures, which increases the rate of oxidative stress and inflammatory products such as cytokines, and ultimately leads to the induction of cell death [24]. Here, the degree of toxicity was observed to be increased as a result of enlarging the applied concentration, which is consistent with the findings of other assessments. Nevertheless, the conduction of in-depth studies is required to obtain a better comprehension on

the real mechanism behind the cytotoxic activity of synthesized nanoparticles.

CONCLUSIONS

This paper introduces an inexpensive, efficient, and fast synthetic path for producing the pure and Ag-dop- α -Fe₂O₃ NPs by extract of *Prosopis farcta* fruit. The traits of synthesized NPs determined by many methods such as XRD, Raman, and FESEM. According to the obtained results, the particle sizes were about 40 and 50 nm for α -Fe₂O₃ and Ag-doped α -Fe₂O₃ NPs, respectively. In addition, the particles were observed to be nearly spherical. According to the hysteresis loop, the saturation magnetization (Ms) of α -Fe₂O₃ and Ag-dop- α -Fe₂O₃ NPs was expressed to be 1.5 and 0.16 emu/g, respectively. The high potential of α -Fe₂O₃ and Ag-dop- α -Fe₂O₃ NPs in performing cytotoxic activities against breast cancer (MCF-7) cells approved by outcomes of MTT. So, the synthesized nanoparticles can be proposed as potential choice for being exerted in advanced medical approaches.

CONFLICT OF INTEREST

The authors report no conflicts of interest in this work.

REFERENCES

- Saeedi, M., et al., Applications of nanotechnology in drug delivery to the central nervous system. *Biomedicine & pharmacotherapy*, 2019. 111: p. 666-675. <https://doi.org/10.1016/j.biopha.2018.12.133>
- Nakhaei, P., et al., Liposomes: structure, biomedical applications, and stability parameters with emphasis on cholesterol. *Frontiers in Bioengineering and Biotechnology*, 2021. 9. <https://doi.org/10.3389/fbioe.2021.705886>
- Fathi Karkan, S., et al., Magnetic nanoparticles in cancer diagnosis and treatment: a review. *Artificial cells, nanomedicine, and biotechnology*, 2017. 45(1): p. 1-5. <https://doi.org/10.3109/21691401.2016.1153483>
- Miri, A., et al., Iron oxide nanoparticles: biosynthesis, magnetic behavior, cytotoxic effect. *ChemistryOpen*, 2021. 10(3): p. 327-333. <https://doi.org/10.1002/open.202000186>
- Mohamed, N.A., et al., Recent Developments in Nanomaterials-Based Drug Delivery and Upgrading Treatment of Cardiovascular Diseases. *International Journal of Molecular Sciences*, 2022. 23(3): p. 1404. <https://doi.org/10.3390/ijms23031404>
- Sanna, V., N. Pala, and M. Sechi, Targeted therapy using nanotechnology: focus on cancer. *International journal of nanomedicine*, 2014. 9: p. 467. <https://doi.org/10.2147/IJN.S36654>
- Miri, A. and M. Sarani, Silver nanoparticles: cytotoxic and apoptotic activity on HT-29 and A549 cell lines. *J. New Develop. Chem.*, 2018. 4: p. 10. <https://doi.org/10.14302/issn.2377-2549.jndc-18-2116>
- Nasirmoghadas, P., et al., Nanoparticles in cancer immunotherapies: An innovative strategy. *Biotechnology progress*, 2021. 37(2): p. e3070. <https://doi.org/10.1002/btpr.3070>
- Wilkinson, L. and T. Gathani, Understanding breast cancer as a global health concern. *The British Journal of Radiology*, 2022. 95(1130): p. 20211033. <https://doi.org/10.1259/bjr.20211033>
- Ghoncheh, M., et al., Epidemiology, incidence and mortality of breast cancer in Asia. *Asian Pacific journal of cancer prevention*, 2016. 17(sup3): p. 47-52. <https://doi.org/10.7314/APJCP.2016.17.S3.47>
- Shakil, M.S., M. Hasan, and S.R. Sarker, Iron oxide nanoparticles for breast cancer theranostics. *Current drug metabolism*, 2019. 20(6): p. 446-456. <https://doi.org/10.2174/1389200220666181122105043>
- Khatami, M., et al., Green Synthesis of Amorphous Iron Oxide Nanoparticles and their Antimicrobial Activity against *Klebsiella pneumoniae*, *Pseudomonas aeruginosa* and *Escherichia coli*. *Iran J Biotechnol*, 2019. 10: p. 33-39.
- Sarani, M., et al., Study of in vitro cytotoxic performance of biosynthesized α -Bi₂O₃ NPs, Mn-doped and Zn-doped Bi₂O₃ NPs against MCF-7 and HUVEC cell lines. *Journal of Materials Research and Technology*, 2022. 19: p. 140-150. <https://doi.org/10.1016/j.jmrt.2022.05.002>
- Kouhbanani, M.A.J., et al., The inhibitory role of synthesized Nickel oxide nanoparticles against Hep-G2, MCF-7, and HT-29 cell lines: the inhibitory role of NiO NPs against Hep-G2, MCF-7, and HT-29 cell lines. *Green Chemistry Letters and Reviews*, 2021. 14(3): p. 444-454. <https://doi.org/10.1080/17518253.2021.1939435>
- Beheshtkhoo, N., et al., Green synthesis of iron oxide nanoparticles by aqueous leaf extract of *Daphne mezereum* as a novel dye removing material. *Applied Physics A*, 2018. 124(5): p. 1-7. <https://doi.org/10.1007/s00339-018-1782-3>
- Mosleh-Shirazi, S., et al., Biosynthesis, simulation, and characterization of Ag/AgFeO₂ core-shell nanocomposites for antimicrobial applications. *Applied Physics A*, 2021. 127(11): p. 1-8. <https://doi.org/10.1007/s00339-021-05005-7>
- Kouhbanani, M.A.J., et al., One-step green synthesis and characterization of iron oxide nanoparticles using aqueous leaf extract of *Teucrium polium* and their catalytic application in dye degradation. *Advances in Natural Sciences: Nanoscience and Nanotechnology*, 2019. 10(1): p. 015007. <https://doi.org/10.1088/2043-6254/aaf74>
- Behzad, F., et al., An overview of the plant-mediated green synthesis of noble metal nanoparticles for antibacterial applications. *Journal of Industrial and Engineering Chemistry*, 2021. 94: p. 92-104. <https://doi.org/10.1016/j.jiec.2020.12.005>
- Veisi, H. and F. Ghorbani, Iron oxide nanoparticles coated with green tea extract as a novel magnetite reductant and stabilizer sorbent for silver ions: Synthetic application of Fe₃O₄@greentea/Agnanoparticles as magnetically separable and reusable nanocatalyst for reduction of 4-nitrophenol. *Applied Organometallic Chemistry*, 2017. 31(10): p. e3711. <https://doi.org/10.1002/aoc.3711>
- Kaur, K. and A.K. Sidhu, Green synthesis: An eco-friendly route for the synthesis of iron oxide nanoparticles. *Frontiers in Nanotechnology*, 2021. 3: p. 47. <https://doi.org/10.3389/fnano.2021.655062>
- Mai, T.T., et al., Ginsenoside F2 induces apoptosis accompanied by protective autophagy in breast cancer stem cells. *Cancer letters*, 2012. 321(2): p. 144-153. <https://doi.org/10.1016/j.canlet.2012.01.045>
- Manke, A., L. Wang, and Y. Rojanasakul, Mechanisms of nanoparticle-induced oxidative stress and toxicity. *BioMed research international*, 2013. 2013. <https://doi.org/10.1155/2013/942916>
- Ankamwar, B., et al., Biocompatibility of Fe₃O₄ nanoparticles evaluated by in vitro cytotoxicity assays using normal, glia and breast cancer cells. *Nanotechnology*, 2010. 21(7): p. 075102. <https://doi.org/10.1088/0957-4484/21/7/075102>
- Wang, L.-S., M.-C. Chuang, and J.-a.A. Ho, Nanotheranostics-a review of recent publications. *International journal of nanomedicine*, 2012. 7: p. 4679. <https://doi.org/10.2147/IJN.S33065>